An Efficient Protocol for CUT&RUN Analysis of FACS-Isolated Mouse Satellite Cells

Kamar Ghaibour, Joe Rizk, Claudine Ebel, Tao Ye, Muriel Philipps, Valérie Schreiber, Daniel Metzger, Delphine Duteil

jove

An Efficient Protocol for CUT&RUN Analysis of FACS-Isolated Mouse Satellite Cells

Kamar Ghaibour[*,1], **Joe Rizk**[*,1], **Claudine Ebel**[1], **Tao Ye**[1], **Muriel Philipps**[1], **Valérie Schreiber**[1], **Daniel Metzger**[1], **Delphine Duteil**[1]

[1] CNRS, Inserm, IGBMC UMR 7104- UMR-S 1258, Université de Strasbourg

[*] These authors contributed equally

Corresponding Author

Delphine Duteil
duteild@igbmc.fr

Citation

Ghaibour, K., Rizk, J., Ebel, C., Ye, T., Philipps, M., Schreiber, V., Metzger, D., Duteil, D. An Efficient Protocol for CUT&RUN Analysis of FACS-Isolated Mouse Satellite Cells. *J. Vis. Exp.* (197), e65215, doi:10.3791/65215 (2023).

Date Published

July 7, 2023

DOI

10.3791/65215

URL

jove.com/video/65215

Abstract

Genome-wide analyses with small cell populations are a major constraint for studies, particularly in the stem cell field. This work describes an efficient protocol for the fluorescence-activated cell sorting (FACS) isolation of satellite cells from the limb muscle, a tissue with a high content of structural proteins. Dissected limb muscles from adult mice were mechanically disrupted by mincing in medium supplemented with dispase and type I collagenase. Upon digestion, the homogenate was filtered through cell strainers, and cells were suspended in FACS buffer. Viability was determined with fixable viability stain, and immunostained satellite cells were isolated by FACS. Cells were lysed with Triton X-100 and released nuclei were bound to concanavalin A magnetic beads. Nucleus/bead complexes were incubated with antibodies against the transcription factor or histone modifications of interest. After washes, nucleus/bead complexes were incubated with protein A-micrococcal nuclease, and chromatin cleavage was initiated with $CaCl_2$. After DNA extraction, libraries were generated and sequenced, and the profiles for genome-wide transcription factor binding and covalent histone modifications were obtained by bioinformatic analysis. The peaks obtained for the various histone marks showed that the binding events were specific for satellite cells. Moreover, known motif analysis unveiled that the transcription factor was bound to chromatin *via* its cognate response element. This protocol is therefore adapted to study gene regulation in adult mice limb muscle satellite cells.

Introduction

Skeletal striated muscles represent on average 40% of the weight of the total human body[1]. Muscle fibers exhibit a remarkable capacity for regeneration upon injury, which is described by the fusion of newly formed myocytes and the generation of new myofibers that replace the damaged ones[2]. In 1961, Alexander Mauro reported a population of mononuclear cells that he termed as satellite cells[3]. These stem cells express the transcription factor paired box 7

(PAX7), and are located between the basal lamina and the sarcolemma of muscle fibers[4]. They were reported to express the cluster of differentiation 34 (CD34; a hematopoietic, endothelial progenitor and mesenchymal stem cell marker), integrin alpha 7 (ITGA7; a smooth, cardiac and skeletal muscle marker), as well as the C-X-C chemokine receptor type 4 (CXCR4; a lymphocyte, hematopoietic, and satellite cell marker)[5]. In basal conditions, satellite cells reside in a particular microenvironment that keeps them in a quiescent state[6]. Upon muscle damage, they become activated, proliferate, and undergo myogenesis[7]. However, contributing only to a minor fraction of the total number of muscle cells, their genome-wide analyses are particularly challenging, especially under physiological settings (<1% of total cells).

Various methods for chromatin isolation from satellite cells have been described, which involve chromatin immunoprecipitation followed by massive parallel sequencing (ChIP-seq) or cleavage under targets and tagmentation (CUT&Tag) experiments. Nevertheless, these two techniques present some significant limitations that remain unchallenged. Indeed, ChIP-seq requires a high amount of starting material to generate enough chromatin, a large proportion of which is lost during the sonication step. CUT&Tag is more appropriate for low cell number, but generates more off-target cleavage sites than ChIP-seq due to the Tn5 transposase activity. In addition, since this enzyme has a high affinity for open-chromatin regions, the CUT&Tag approach might be preferentially used for analyzing histone modifications or transcription factors associated with actively transcribed regions of the genome, instead of silenced heterochromatin[8,9].

Presented here is a detailed protocol that allows the isolation of mouse limb muscle satellite cells by FACS for cleavage under targets and release using nuclease (CUT&RUN)[10,11] analysis. The various steps involve the mechanical disruption of tissue, cell sorting, and nuclei isolation. The method's efficiency, regarding the preparation of a viable cell suspension, was demonstrated by performing CUT&RUN analysis for covalent histone modifications and transcription factors. The quality of isolated cells makes the described method particularly attractive for preparing chromatin that captures the native genomic occupancy state faithfully, and is likely to be suitable for capturing the chromosome conformation in combination with high-throughput sequencing at specific loci (4C-seq) or at genome-wide levels (Hi-C).

Protocol

Mice were kept in an accredited animal house, in compliance with National Animal Care Guidelines (European Commission directive 86/609/CEE; French decree no.87-848) on the use of laboratory animals for research. Intended manipulations were submitted to the Ethical committee (Com'Eth, Strasbourg, France) and to the French Research Ministry (MESR) for ethical evaluation and authorization according to the 2010/63/EU directive under the APAFIS number #22281.

1. Preparation of cell suspension for isolation of satellite cells by fluorescence-activated cell sorting (FACS) (Figure 1)

1. Isolation of muscle tissue
    1. Decontaminate the tools for muscle dissection, including forceps, scalpels, and scissors, using a cleaning agent (**Table 1**), and rinse thoroughly with distilled water.

2. Prepare two 2 mL tubes (**Table 1**), each containing 1 mL of muscle isolation buffer, and place them on ice for collecting harvested muscles.

3. Sacrifice two 10-week-old C57/Bl6J male mice by CO_2 asphyxiation followed by cervical dislocation. Spray 70% ethanol over each entire mouse. Peel off the skin from the hind limb using forceps. Dissect out all the limb muscles surrounding the femur, tibia, and fibula (approximately 1 mg of muscles per mouse).
NOTE: The satellite cells number decreases after 15 weeks of age.

4. Place the harvested limb muscles into 2 mL tubes containing 1 mL of muscle isolation buffer prepared in step 1.1.2. Collect the muscles from the second mouse following the same procedure. Mince the harvested muscles with scissors on ice until smaller than 1 mm^3 fragments are obtained.
NOTE: Muscles were collected and minced mainly as described[12]. Perform tissue digestion either following step 1.2 or 1.3.

2. Tissue digestion with collagenase enzyme

1. Transfer the minced muscle suspension from the two mice by pouring them into a 50 mL tube (**Table 1**) containing 18 mL of muscle isolation buffer (supplemented with 5 mL [5 U/mL] of dispase and 5 mg of type I collagenase) (**Table 1**).

2. Close the tube tightly and seal it with laboratory film (**Table 1**). Place it horizontally in a shaking water bath (**Table 1**) at 37 °C at 100 rpm for 30 min.

3. After 30 min, add 5 mg of type I collagenase. Keep tubes for another 30 min under agitation in a shaking water bath at 37 °C at 100 rpm.

4. Upon digestion, pipette the muscle suspension up and down 10 times with a 10 mL pipette to improve the efficiency of dissociation. Centrifuge at 4 °C at 400 x *g* for 5 min. A clear pellet will be visible at the bottom of the tube. Discard the supernatant using a 10 mL pipette, leaving 5 mL of medium in the tube.
NOTE: Leaving the medium helps avoid stressing the cells. Add 10 mL of fresh muscle isolation buffer and resuspend the pellet by pipetting up and down with a 10 mL pipette.

5. Place 100 µm, 70 µm, and 40 µm cell strainers (one of each kind) (**Table 1**) on open 50 mL tubes. Pipette the suspension onto the successive cell strainers (100 µm, 70 µm, 40 µm) and collect the flowthrough into the 50 mL tubes, containing cells below 40 µm.

6. Centrifuge the suspension at 4 °C at 400 x *g* for 5 min. Discard the supernatant using a 10 mL pipette until 2 mL remain, and then use a 0.2-1 mL pipette until 100-200 µL remain. Resuspend the pellet in 2 mL of red blood cell lysis buffer (**Table 2**). Incubate on ice for 3 min.

7. Centrifuge at 4 °C at 400 x *g* for 5 min and discard the supernatant using a 20-200 µL pipette. Resuspend the cells in 100 µL of cold FACS buffer (**Table 2**). Place on ice.

3. Alternative method for tissue digestion with Liberase thermolysin low (TL) enzyme

1. Follow the descriptions in step 1.1. for tissue isolation.

2. For Liberase-mediated tissue disaggregation, harvest muscles in 2 mL of Roswell Park Memorial Institute (RPMI) isolation buffer (**Table 2**), instead of muscle isolation buffer described in step 1.1.2.

3. Transfer the minced muscle suspension from the two mice by pouring them into a 50 mL tube (**Table 1**) containing 18 mL of RPMI isolation buffer supplemented with 300 or 600 µL of Liberase TL at 5 mg/mL (**Table 1**) (i.e., 0.083 mg/mL and 0.167 mg/mL final concentrations, respectively)[13].
4. Close the tube tightly and seal it with laboratory film (**Table 1**). Place it horizontally in a shaking water bath (**Table 1**) at 37 °C at 100 rpm for 30 min.
5. Upon digestion, pipette the muscle suspension up and down 10 times with a 10 mL pipette to dissociate and improve the efficiency of dissociation.
6. Centrifuge at 4 °C at 400 x *g* for 5 min. A clear pellet will be visible at the bottom of the tube. Discard the supernatant using a 10 mL pipette, leaving 5 mL of medium in the tube. Leaving the medium helps avoid stressing the cells. Add 10 mL of fresh RPMI isolation buffer, and resuspend the pellet by pipetting up and down with a 10 mL pipette.
7. Place 100 µm, 70 µm, and 40 µm cell strainers (one of each kind) (**Table 1**) on open 50 mL tubes.
8. Pipette the suspension onto successive cell strainers (100 µm, 70 µm, 40 µm) and collect the flowthrough into the 50 mL tubes, containing cells below 40 µm.
9. Centrifuge the suspension at 4 °C at 400 x *g* for 5 min. Discard the supernatant using a 10 mL pipette until 2 mL remain, and then use a 0.2-1 mL pipette until 100-200 µL remain.
10. Resuspend the pellet in 2 mL of red blood cell lysis buffer (**Table 2**). Incubate on ice for 3 min.
11. Centrifuge at 4 °C at 400 x *g* for 5 min and discard the supernatant using a 20-200 µL pipette.
12. Resuspend the cells in 100 µL of cold FACS buffer (**Table 2**). Place on ice.

4. Preparation of cell suspension for FACS isolation
    1. Transfer 10 µL of the cell suspension obtained in step 1.2.12 into a fresh 1.5 mL tube. This sample will constitute the unstained control or the negative control (**Figure 2**). Add 190 µL of FACS buffer, transfer to a 5 mL tube (**Table 1**), and store on ice.
    2. Centrifuge the remaining 90 µL of the cell suspension obtained in step 1.2.12 at 4 °C at 400 x *g* for 5 min and discard the supernatant using a pipette (20-200 µL tip volume). Incubate the cells with 400 µL of fixable viability stain (**Table 3**) diluted in serum-free Dulbecco's modified Eagle medium (DMEM) for 15 min at room temperature (RT).
    3. Wash the cells by centrifugation at 4 °C at 400 x *g* for 5 min and add 100 µL of FACS buffer. Gently invert the tubes three times and centrifuge again at 4 °C at 400 x *g* for 5 min.
    4. During the centrifugation time, prepare 100 µL of a master mix of primary antibodies coupled to fluorophores and directed against CD11b, CD31, CD45, TER119, CD34, ITGA7, and CXCR4 (**Table 3**), diluted in FACS buffer.
    5. Centrifuge at 400 x *g* for 5 min at 4 °C, discard the cell supernatant using a pipette (20-200 µL tip volume), and add the 100 µL antibody mix. Gently invert the tube three times. Do not vortex. Incubate in the dark on ice for 30 min.

6. Centrifuge at 400 x *g* for 5 min at 4 °C. Discard the supernatant using a 20-200 µL pipette and add 500 µL of 1x phosphate-buffered saline (PBS) to wash the cells. Gently invert the tube three times. Re-centrifuge at 400 x *g* for 5 min at 4 °C and discard the supernatant using a 20-200 µL pipette.

7. Resuspend the cell pellet in 500 µL of FACS buffer and transfer the suspension to a 5 mL tube.
   NOTE: the cell suspension obtained from Liberase digestion is processed in the same way.

5. Satellite cells selection by FACS

   1. Briefly vortex the cell suspension (2-5 sec) and process the cells on a flow cytometer equipped with a 100 µm nozzle (**Table 1**).

   2. Determine the various gate sizes based on the unstained sample stored at step 1.4.1 (**Figure 2**).

   3. Coat a 5 mL tube with 1 mL of pure fetal calf serum (FCS) to improve cell collection and add 500 µL of FACS buffer.

   4. Exchange the unstained sample with the antibody-labelled sample.

   5. Select the population of interest according to the forward scatter area (FSC-A) and side scatter area (SSC-A) (**Figure 3A**), and remove doublet cells with the FSC-A and forward scatter height (FSC-H) (**Figure 3B**)[14].

   6. Identify living cells with fixable viability stain negative staining (**Figure 3C**).

   7. Select negative cells for CD31, CD45, TER119, and CD11b (**Figure 3D**).

   8. To identify satellite cells, select first the cells that are positive for CD34 and ITGA7 (**Figure 3E**), and then select the CXCR4-positive cells on the CD34- and ITGA7-selected population (**Figure 3F**).

   9. Collect the selected cells (between 40,000 and 80,000 cells, according to the quality of the preparation) in the 5 mL coated tube containing 500 µL of FACS buffer.

2. Validation of the isolated population in tissue culture

1. Slide coating with hydrogel

   1. Dilute 280 µL of a pure hydrogel human embryonic stem cell (hESC) qualified matrix (**Table 1**) in 12 mL of serum-free DMEM/F12 medium.

   2. Coat a chamber slide (**Table 1**) with the hydrogel solution, and incubate it overnight at 4 °C.

   3. The next day, incubate the chamber slide at 37 °C and 5% CO_2 for 1 h before cell seeding.

2. Cell growth and differentiation

   1. Plate out approximately 20,000 cells, obtained from step 1.5.9, per well, and grow them in growth medium (**Table 2**) for 5 days. Take phase-contrast images using a brightfield microscope (**Figure 4A**), before processing them for immunofluorescence analysis to ensure the quality of the preparation (**Figure 4B**).

   2. To induce myogenesis, grow amplified satellite cells from step 2.2.1 in myogenic medium (**Table 2**) for an additional 7 days. Take phase-contrast images using brightfield microscope (**Figure 4C**) before processing them for immunofluorescence analysis to ensure the quality of the preparation (**Figure 4D**).

3. Immunocytofluorescence analysis

1. Gently remove the medium, wash the cells that were cultured on chamber slide with 100 µL of 1x PBS twice, and fix them with 100 µL of 4 % paraformaldehyde (PFA) at RT for 1 h.

   NOTE: This step should be performed with care. A small volume of medium should always be kept in the chamber to prevent stressing the cells, and the PBS should be poured through the walls of the chamber.

2. Wash the cells three times with 100 µL of 1x PBS, supplemented with 0.1% Tween 20 (PBST) to permeabilize the cell membranes.

3. Block unspecific signals by incubation in 100 µL of 1x PBST supplemented with 5% FCS (PBST-FCS) at RT for 1 h.

4. Incubate the cells with 100 µL of a master mix of anti-PAX7 and anti-dystrophin (DMD) antibodies (diluted in 1x PBST-FCS) at 4 °C overnight, to detect satellite cells and myofibers, respectively.

5. Wash the cells three times with 100 µL of 1x PBST, and incubate them with 100 µL of goat anti-mouse Cy3 or goat anti-rabbit Alexa 488 secondary antibodies (**Table 3**) diluted in 1x PBST-FCS at RT for 1 h.

6. Dissociate the chamber wells from the slide using the equipment provided by the supplier, add 20 µL of aqueous mounting medium with 4′,6-diamidino-2-phenylindole (DAPI), and cover the slide with a coverslip (**Table 1**).

7. Observe and capture the image of the stained cells with a confocal microscope.

8. Process the images using image analysis software (**Figures 4B,D**).

3. CUT&RUN analysis

1. Sample preparation for CUT&RUN analysis on FACS-isolated satellite cells

   NOTE: CUT&RUN was performed essentially as described[10,15]. The buffer composition is presented in **Table 2**.

   1. For the CUT&RUN assay, use approximately 40,000 of the cells obtained in method 1, step 1.5.9, per sample/antibody that must be tested.

   2. Centrifuge the FACS-isolated satellite cells at RT at 500 x *g* for 10 min, then discard the supernatant using a pipette (20-200 µL tip volume).

   3. Wash the cells with 1 mL of 1x PBS, centrifuge at RT at 500 x *g* for 5 min, discard the supernatant using a pipette (0.2-1 mL tip volume), and resuspend them in 1 mL of cold nuclear extraction buffer (**Table 2**). Incubate on ice for 20 min.

   4. During incubation, prepare one 1.5 mL tube containing 850 µL of cold binding buffer (**Table 2**) and add 20 µL of concanavalin A-coated magnetic beads per sample (**Table 1**).

   5. Wash the beads twice with 1 mL of cold binding buffer using a magnetic rack (**Table 1**). For each wash or buffer change throughout the procedure, let the beads accumulate at the side of the tube on the magnetic rack for 5 min before removing the cleared supernatant with a pipette (0.2-1 mL tip volume). Then, resuspend gently in 300 µL of cold binding buffer.

6. Centrifuge the nuclei at 4 °C at 600 x *g* for 5 min and resuspend them gently in 600 µL of nuclear extraction buffer. Gently mix the 600 µL of extracted nuclei with the 300 µL of concanavalin A bead slurry, and incubate at 4 °C for 10 min.

7. Remove the supernatant using a magnetic rack, as described in step 3.1.4, and resuspend the bead-bound nuclei gently with 1 mL of cold blocking buffer (**Table 2**). Incubate at RT for 5 min.

8. Remove the supernatant using a magnetic rack and wash the bead-bound nuclei twice with 1 mL of cold wash buffer (**Table 2**). During the second wash, equally split the bead-bound nuclei into 1.5 mL tubes. Each tube will be treated with a specific antibody in the following step.
   NOTE: In this example, 250 µL of bead-bound nuclei were split in four 1.5 mL tubes.

9. Separate the supernatant using a magnetic rack, as described in step 3.1.4, and aspirate with a pipette. Gently resuspend the nucleus/bead complexes with a specific primary antibody (**Table 3**), or an IgG of another species (here rabbit) diluted in 250 µL of cold wash buffer. Incubate at 4 °C overnight with gentle agitation.
   NOTE: The antibodies used here are directed against AR, H3K4me2, and H3K27ac.

10. Remove the supernatant with a magnetic rack, as described in step 3.1.4, wash the bead-bound nuclei twice with 1 mL of cold wash buffer, and resuspend in 100 µL of cold wash buffer.

11. Dilute protein A-micrococcal nuclease at 1.4 ng/µL in 100 µL per sample of cold wash buffer.

12. Add 100 µL of protein A-micrococcal nuclease to the 100 µL of sample obtained in 3.1.11 and incubate at 4 °C for 1 h with agitation.

13. Remove the supernatant with a magnetic rack, as described in step 3.1.4, wash twice with 1 mL of cold wash buffer, and resuspend the bead-bound nuclei in 150 µL of cold wash buffer.

14. To initiate DNA cleavage, add 3 µL of 100 mM of $CaCl_2$ to the 150 µL of sample, mix quickly by flicking, and incubate on ice for 30 min. Stop the reaction by adding 150 µL of stop buffer and incubate at 37 °C for 20 min to digest the RNA and release the DNA fragments.

15. For DNA extraction, centrifuge the samples at 16,000 x *g* at 4 °C for 5 min.

16. Transfer the supernatant to a new microfuge tube and discard the pellet and beads.

17. Add 3 µL of 10% sodium dodecyl sulfate (SDS) and 2.5 µL of 20 mg/mL proteinase K. Mix by inversion. Incubate for 10 min at 70 °C (no shaking).

18. Add 300 µL of phenol/chloroform/isoamyl alcohol, vortex, transfer to 2 mL phase-lock tubes (pre-spinned for 5 min at 16,000 x *g*), and centrifuge for 5 min at 16,000 x *g* at 4 °C.

19. Add 300 µL of chloroform to the same tube and centrifuge for 5 min at 16,000 x *g* at 4 °C. Collect the supernatant (~300 µL) with a pipette (0.2-1 mL tip volume) and transfer into a new 1.5 mL tube.

20. Add 1 µL of glycogen (20 mg/mL concentration).

21. Add 750 µL of 100% ethanol and precipitate overnight at -20 °C.

22. Pellet the DNA by centrifugation for 15 min at 16,000 x *g* at 4 °C. Wash the pellet with 1 mL of 100% ethanol, centrifuge for 5 min at 16,000 x *g*, discard the supernatant, centrifuge for 30 s at 16,000 x *g*, and remove the liquid with a pipette (20-200 µL tip volume).
23. Air-dry the pellet for ~5 min. Resuspend in 25 µL of 1 mM Tris-HCl (pH 8) and 0.1 mM ethylenediaminetetraacetic acid (EDTA; pH 8).

2. Bioinformatics analysis
    1. Prepare libraries from immunocleaved DNA and sequence them as paired-end 100 bp reads with the help of the genomic platform as described[16].
    2. Remove reads overlapping with the ENCODE blacklist region (V2) and separate the remaining reads into two groups: fragment size <120 bp (without nucleosome, in general for transcription factors) and fragment size >150 bp (with nucleosomes, normally for histone marks). Map to the mm10 reference genome using Bowtie 2 (v2.3.4.3)[17].
    3. Generate bigwig files with bamCoverage (deeptools 3.3.0: bamCoverage --normalizeUsing RPKM --binSize 20).
    4. Retain uniquely mapped reads for further analysis.
    5. Generate raw bedgraph files with genomeCoverageBed (bedtools v2.26.0).
    6. Use the SEACR 1.3 algorithm (stringent option) for the peak calling. Load the target data bedgraph file in UCSC bedgraph format that omits regions containing zero signal, and control (IgG) data bedgraph file to generate an empirical threshold for peak calling[18].
    7. Perform a Pearson correlation analysis with deeptools to determine the similarity between the samples[19]. Use the command line multiBamSummary bins --bamfiles file1.bam file2.bam -o results.npz, followed by plotCorrelation -in results.npz --corMethod pearson --skipZeros --plotTitle "Pearson Correlation of Read Counts" --whatToPlot heatmap --colorMap RdYlBu --plotNumbers -o heatmap_PearsonCorr_readCounts.png --outFileCorMatrix PearsonCorr_readCounts.tab.
    8. Visualize the genome-wide intensity profiles with IGV[20] using bedgraph files and the bed file peaks obtained from SEACR.
    9. Use HOMER for peak annotation and motif search[21].
    10. Finally, compare the datasets with previously published ones with ChIP-Atlas Peak browser to visualize them on IGV, and/or enrichment analysis using the SEACR-generated bed files as an input dataset[22].

Representative Results

Satellite cells from mouse skeletal muscles were isolated by combining the protocols of Gunther et al. (hereafter Protocol 1)[12] and of Liu et al.[23] (hereafter Protocol 2). Since non-digested muscle fibers were observed after digestion when using the concentration of collagenase and dispase proposed in Protocol 1, the quantity of enzymes was increased to improve muscle fiber dissociation, as described in steps 1.2.1 and 1.2.3. As indicated in Protocol 2, the samples were

subjected to a gentle agitation in a water bath to maintain cell viability. We performed filtration through cell strainers, as mentioned in Protocol 1, and incubation with red blood cell lysis buffer (see steps 1.2.7 to 1.2.10). In Protocol 1, cells were loaded on a Percoll density gradient of 30%/70% to isolate mononucleated cells at the interphase, which may have led to the loss of cells of interest. Thus, this step was omitted, as proposed in Protocol 2.

FSC-A versus SSC-A gating was used to identify mononucleated cells based on size (FSC) and granularity (SSC) (**Figure 3A**). Debris were excluded by ignoring events below 40 K on the FSC-A axis, and 38.8% ± 3.6% of cells were selected. FSC-A versus forward scatter height (FSC-H) gating density plots were used for doublet exclusion (**Figure 3B**). After selecting the cells negative for the fixable viability stain marker, an average of 34.3% ± 7.7% of live cells was obtained (**Figure 3C**).

The percentage shown in the dot plot in **Figure 3C**, 75.4%, corresponds to the percentage of single living cells, calculated from the parent cell population, which is in this case the singles. 95.7% of single cells are obtained from the live events which make up 35% of the total events. Thus, the percentage 34.3% obtained on average, is calculated from the total events and not the parent populations.

About 3% of single living cells were negative for leukocyte- (CD45), monocyte- (CD11b), endothelial- (CD31), and erythroid-specific (TER119) markers (**Figure 3D**). CD11b/CD45/CD31/TER119 negative cells were then selected according to their expression of CD34 (hematopoietic, endothelial progenitors, and mesenchymal stem cells) and ITGA7 (cardiac, smooth, and skeletal muscle cells) markers (**Figure 3E**). A final gating for CXCR4 (lymphocytes, hematopoietic, and satellite cells) was performed to select putative satellite cells (**Figure 3F**). From the CD34+/ITGA7+ cells, ~80% were found to be positive for CXCR4, which represents an average of 1% ± 0.15% of total single living cells, and an absolute number of 60,000 ± 14,000 putative satellite cells per mouse limb muscles among 14 independent experiments. An additional resorting assessment on the CXCR4+ cell fraction revealed that about 80% of living cells were obtained after post-sorting, of which almost 70% were CXCR4+ (**Figure S1**), showing the high viability and purity of this FACS-isolated cell population.

Since various studies compared the efficiency of collagenase and Liberase TL enzymes for cell isolation[24,25], these two digestion methods have been processed in parallel. With 300 µL of Liberase TL, the digestion was less efficient than with collagenase, as undigested fibers remained. In addition, more cell debris and large events were observed (**Figures S2A,B**), and only 17.3% of single living cells on average were obtained after FVS 780 selection (**Figure S2C**). An additional concern with Liberase digestion was the low number of CD34+/ITGA7+ cells compared to collagenase (**Figures S2D-S2E**), even though CXCR4 gating was similar (**Figure S2F**). With 600 µL of Liberase TL, the digestion was more efficient. However, the amount of cell debris remained elevated and the cell viability substandard (16.3%) (**Figure S3**). Thus, digestion with Liberase TL was less efficient for satellite cell isolation.

When seeded, more than 70% of the CD34+/ITGA7+/CXCR4+ cells (**Figure 4A**) expressed PAX7 (**Figure 4B**), contrary to CD34+/ITGA7-/CXCR4- cells that were PAX7-negative (**Figure 4C**). CD34+/ITGA7+/CXCR4+ cells were able to differentiate into myofibers when grown in a myogenic medium for 7 additional days, as shown by dystrophin (DMD) staining (**Figure 4D**), confirming their

myogenic potential. Thus, combined tissue culture and immunofluorescence analyses showed that FACS-isolated CD34+/ITGA7+/CXCR4+ cells are satellite cells.

To determine whether isolated satellite cells are suitable for CUT&RUN analysis, the genomic profile of acetylated lysine 27 (H3K27ac) and dimethylated lysine 4 (H3K4me2) of histone H3, two histone modifications found at active promoter and enhancer regions, was determined. Our data uncovered 68,694 and 13,514 peaks for H3K4me2 and H3K27ac, respectively, with a similar genomic repartition between the two histone marks (**Figure S4A**). In detail, we found that one-quarter of the peaks were located ± 2 kb from the transcription start site (TSS) of the nearest gene, the majority being located either -100 kb to -10 kb, or 10 kb to 100 kb from the TSS (**Figure S4B**). Of note, Pearson analysis showed an 80% correlation between H3K27ac and H3K4me2 read profiles (**Figure S4C**). To assess that the chromatin prepared from the abovementioned protocol was isolated from satellite cells, the presence of H3K27ac and H3K4me2 at the promoter of satellite cell-specific genes was determined. H3K4me2 was enriched around the TSS of *Pax7*, *Itga7*, *Lamb2*, *Cxcr4*, and *Vcam1* (**Figure 5A**), but not at those of *Itgam* (CD11b) and *Ptprc* (CD45) (immune cells), *Pecam* (CD31; endothelial cells) (**Figure 5B**), *Ckm* (developing muscle fibers), or *Myh3* (myosin heavy chain fast embryonic, myofibers) (**Figure 5C**). Similar results were obtained with H3K27ac (**Figure 5**). Almost no signal was obtained with the IgG sample (**Figure 5**). Moreover, comparison of the H3K27ac peaks obtained from SEACR with those resulting from MACS2 peak calling from published ChIP-seq datasets showed a high correlation, as noted below each panel (ChIP-Atlas track; **Figure 5**). Together, these results indicate that the reads obtained after the bioinformatics analysis originate from the chromatin of FACS-isolated satellite cells and correlate with those previously identified by ChIP-seq analyses.

While single-cell RNA sequencing studies in mouse satellite cells showed a striking stress response, caused by the isolation procedure[26], the presence of H3K4me2 or H3K27ac was determined at stress response genes, as exemplified with *Atf3*, *Azin1*, *Gls*, and *Elf2*. The results provide evidence that the H3K27ac mark is not deposited at the promoter of such genes, and that levels of H3K4me2 remain low compared to those obtained for satellite cell-specific genes (**Figure S5**). Thus, these data highlight how mild the isolation procedure is.

Next, the suitability of our isolation method for transcription factors was examined. CUT&RUN analysis for the androgen receptor (AR), a transcription factor that belongs to the nuclear receptors superfamily and that plays an important role in myogenic differentiation[27], unraveled 7,840 peaks. These peaks were mainly located at intron and intergenic regions (**Figure S4A**), either -100 kb to -10 kb, or 10 kb to 100 kb from the TSS (**Figure S4B**). Phylogenetic analyses revealed that AR, alongside the glucocorticoid (*GR/Nr3c1*), the mineralocorticoid (*MR/Nr3c2*), and the progesterone (*PR/Nr3c3*) receptors, is a member of the oxosteroid nuclear receptors subfamily[28], that bind as homodimers to DNA segments which are made up of two 5′-RGAACA-3′ palindromic half-sites separated by three base pairs[29]. Searching for a known motif by means of hypergeometric optimization of motif enrichment (HOMER, http://homer.ucsd.edu/homer/) revealed that AR is bound to the 5′-RGRNCA-3′ AR half-site motif, to the typical 5′-RGNACAnnnTGTNC-3′ oxosteroid motif (referred in the figure as PR), and to the 5′-RGNACAnnnTGTNCY-3′ AR consensus motif in >32%, 17%, and 2% of the targeted

regions, respectively (**Figure 6A**). It should be noted that similar proportions were previously obtained for the glucocorticoid receptor in skeletal muscle[16].

SEACR analysis unveiled almost 500 peaks with a peak score >50, with more than 200 of them with a score >100; some of which are exemplified in **Figure 6B**. Our analysis also uncovered a modest enrichment of AR at the previously described binding sites of genes involved in polyamine biosynthesis (*Amd1*, *Oat*, and *Smox*) and in prostate cancer (*Acox1*, *Fkbp5*, and *Tmprss2*) (**Figure S6**). Interestingly, the AR was found at the loci of genes involved in satellite cell stemness (*Pax7*, *Cxcr4*, and *Cd34*) (**Figure S7**). Of note, the oxosteroid response element was found at each of these AR-enriched regions (**Figure S6** and **Figure S7**), demonstrating that the AR signal seen in the CUT&RUN data is highly specific.

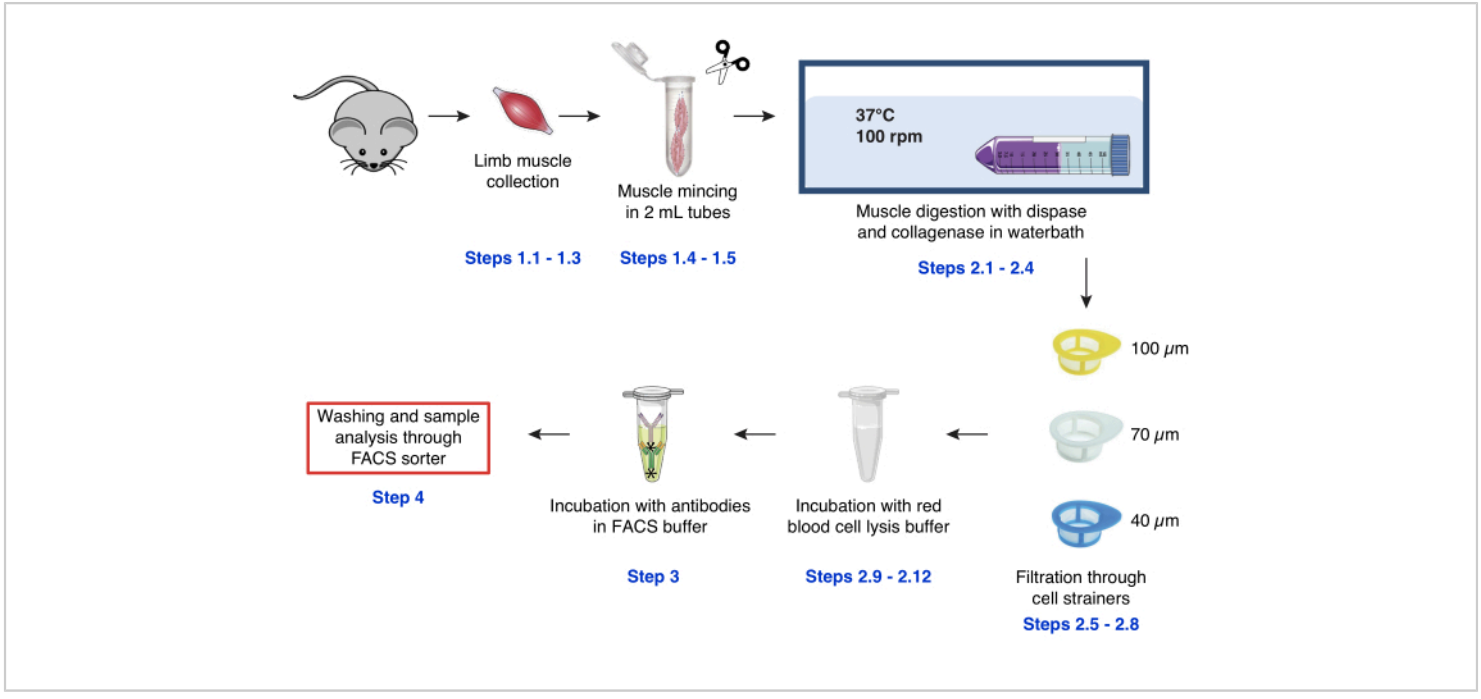

Figure 1: Schematic representation of the protocol used for satellite cell isolation from mouse limb muscles. The protocol comprises four mains steps. Briefly, mice are sacrificed, and the hind limb muscles are harvested (steps 1.1.1-1.1.3) and mechanically minced using scissors (steps 1.4-1.5). This is followed by steps 1.2.1-1.2.4, during which muscles are dissociated in a water-bath using collagenase and dispase. In steps 1.2.5-1.2.8, the cell suspension is filtered through 100, 70, and 40 µm cell strainers, consecutively, and erythrocytes are eliminated using red blood cell lysis buffer (steps 1.2.9-1.2.12). The remaining cell populations are labelled in step 1.3 with antibodies coupled to fluorophores, which are directed against specific cellular phenotypical markers. Step 1.4 includes samples passing through FACS to collect satellite cells for further application. Please click here to view a larger version of this figure.

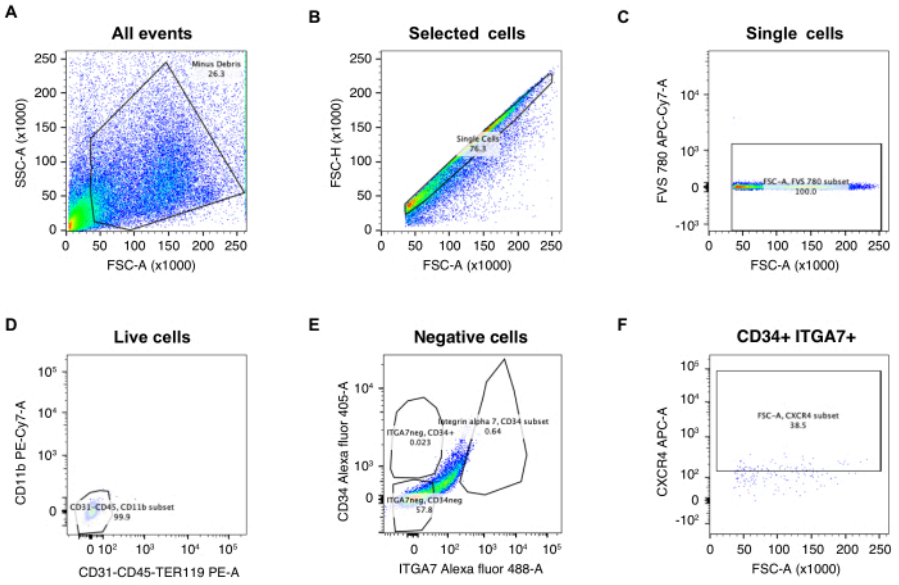

Figure 2: Flow cytometry analysis of an unstained cell preparation. (**A**) Selection of the population of interest based on FSC-A and SSC-A parameters. (**B**) Single cell identification based on FSC-A and FSC-H. (**C**) Characterization of the auto-fluorescence threshold of collected cells for APC-Cy7 conjugated to the fixable viability stain (FVS 780) marking dead cells. (**D-F)**. Auto-fluorescence measurement for PE-Cy7 conjugated to CD11b antibody and PE-conjugated to TER119/CD45/CD31 markers (**D**), as well as for Alexa fluor 488 conjugated to ITGA7, Alexa fluor 405 conjugated to CD34 (**E**), and APC fluorochrome conjugated to CXCR4 (**F**). Gates are represented as black boxes. Please click here to view a larger version of this figure.

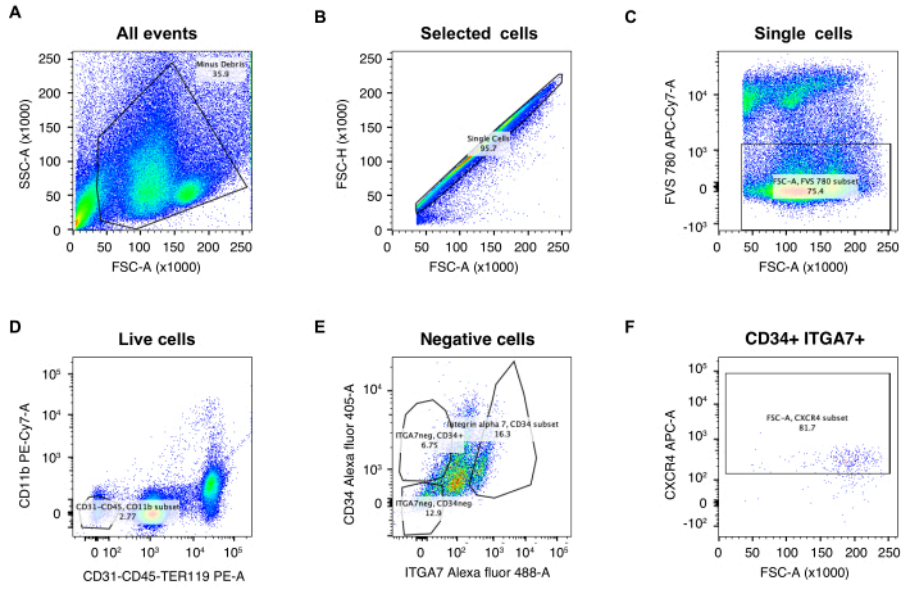

Figure 3: Flow cytometer gating strategy for satellite cell sorting. (**A**) Selection of the population of interest based on FSC-A and SSC-A parameters. (**B**) Single cell identification based on FSC-A and FSC-H. (**C**) Identification of living cells with FVS 780. (**D**) Negative cell selection based on CD11b, CD31, CD45, and TER119 antigens. (**E-F**) Positive cell selection based on CD34 and ITGA7 (**E**), as well as CXCR4 (**F**) antigens. Gates are represented as black boxes. Please click here to view a larger version of this figure.

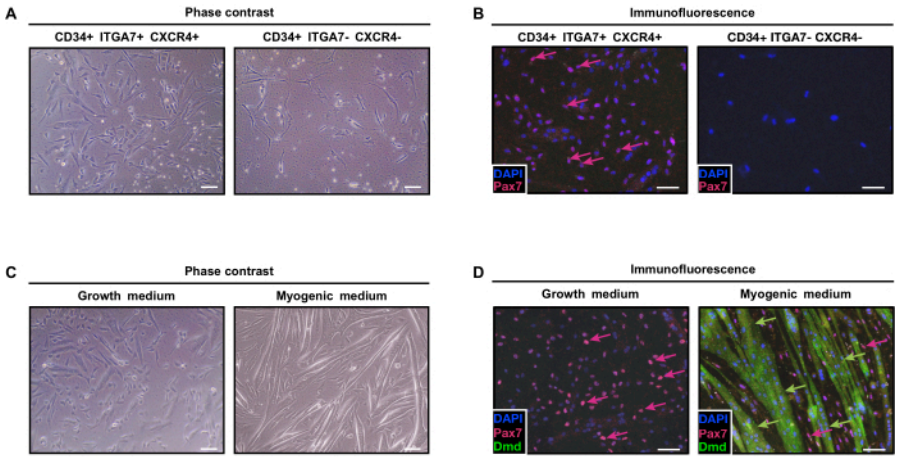

Figure 4: Analysis of FACS-isolated CD34+/ITGA7+/CXCR4+ and CD34+/ITGA7-/CXCR4- cells. (**A**) Phase contrast images of CD34+/ITGA7+/CXCR4+ and CD34+/ITGA7-/CXCR4- cells cultured in growth medium. (**B**) Immunofluorescence analysis of CD34+/ITGA7+/CXCR4+ and CD34+/ITGA7-/CXCR4- cells cultured in growth medium using antibodies directed against PAX7 (red) and dystrophin (DMD, green). Nuclei were stained with DAPI (blue). Magenta arrows indicate PAX7-positive cells. (**C**) Phase contrast images of CD34+/ITGA7+/CXCR4+ cells grown for 5 days in growth medium (left panel) and for 7 additional days in myogenic medium (right panel). (**D**) Immunofluorescence analysis images of CD34+/ITGA7+/CXCR4+ cells grown for 5 days in growth medium (left panel) and for 7 additional days in myogenic medium (right panel) using antibodies directed against PAX7 (red) and dystrophin (DMD, green). Nuclei were stained with DAPI (blue). Magenta arrows indicate PAX7-positive cells. Green arrows indicate DMD-positive cells. Scale bars: brightfield panels = 25 µm; immunofluorescence panels = 50 µm. Please click here to view a larger version of this figure.

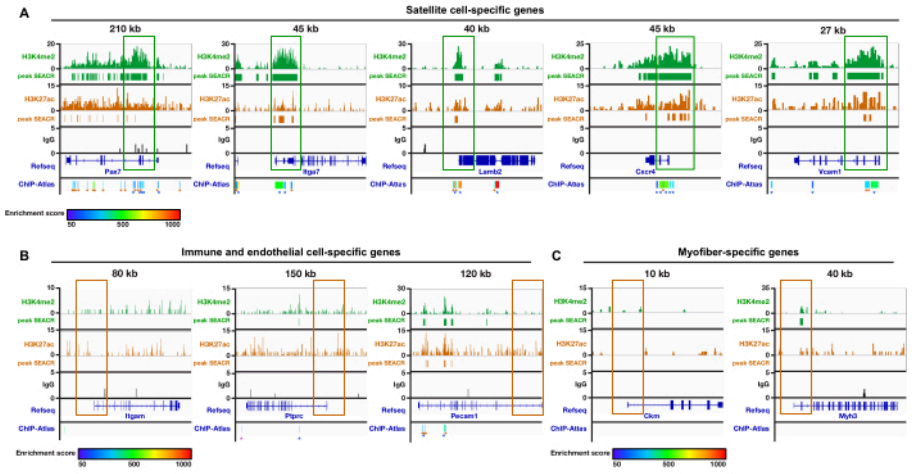

Figure 5: Genomic profiles of satellite cell chromatin. Localization of H3K4me2 and H3K27ac at satellite cell-specific genes (**A**), immune and endothelial cell-specific genes (**B**), and myofiber-specific genes (**C**) on the chromatin of satellite cells by CUT&RUN. Active promoters are boxed in green, whereas inactive promoters are boxed in brown. CUT&RUN performed with IgG was used as a negative control. H3K27ac enrichment analysis for histone marks is presented below each track. Enrichment score showing the levels of confidence of published datasets is depicted as a heatmap. Brown stars (*) refer to H3K27ac ChIP-seq peaks performed in muscle satellite cells, blue stars to H3K4me3, and the pink one to H4K16me1.

Please click here to view a larger version of this figure.

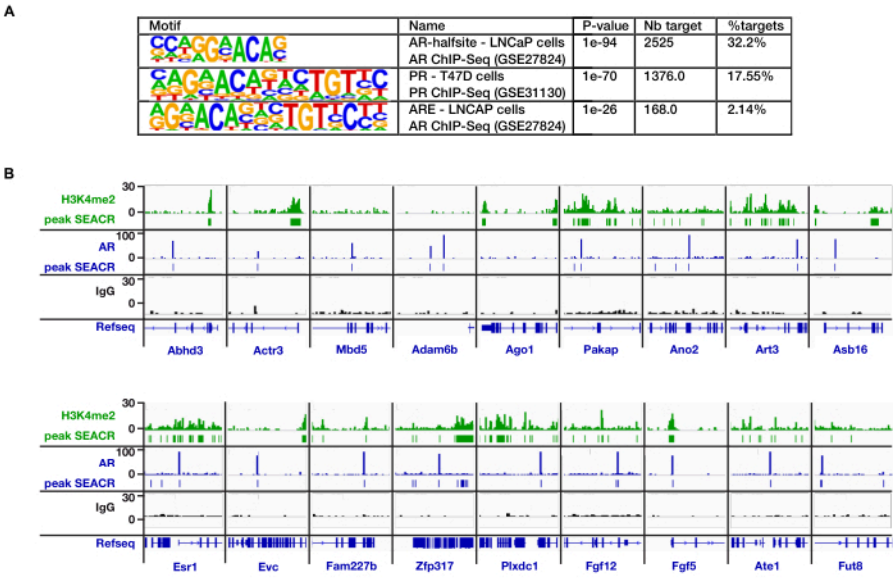

Figure 6: AR genomic distribution on satellite cell chromatin. (**A**) HOMER-known motif analysis of AR peaks in satellite cells. PR: progesterone receptor. Nb target refers to the number of peaks presenting a particular motif. (**B**) Localization of H3K4me2 and AR at indicated genes on the chromatin of satellite cells determined by CUT&RUN. CUT&RUN performed with IgG was used as a negative control. Please click here to view a larger version of this figure.

Table 1: List of materials, reagents, and software. Please click here to download this Table.

Table 2: Buffer compositions. Please click here to download this Table.

Table 3: Antibody references and concentrations. Please click here to download this Table.

Supplementary Figure 1: Flow cytometry analysis of the cell preparation post-sorting. (**A**) Selection of the population of interest based on FSC-A and SSC-A parameters. (**B**) Single cell identification based on FSC-A and FSC-H. (**C**) Identification of living cells with fixable viability stain (FVS 780). (**D**) Negative cell selection based on CD11b, CD31, CD45, and TER119 antigens. (**E-F**) Positive cell selection based on CD34 and ITGA7 (**E**) as well as CXCR4 (**F**) antigens. Gates are represented as black boxes. Please click here to download this File.

Supplementary Figure 2: Flow cytometer gating strategy for satellite cell sorting after digestion with 300 µL of Liberase TL. (**A**) Selection of the population of interest based on FSC-A and SSC-A parameters. (**B**) Single cell identification based on FSC-A and FSC-H. (**C**) Identification of living cells with FVS 780. (**D**) Negative cell selection based on CD11b, CD31, CD45, and TER119 antigens. (**E-F**) Positive cell selection based on CD34 and ITGA7 (**E**) as well as CXCR4 (**F**) antigens. Gates are represented as black boxes. Please click here to download this File.

Supplementary Figure 3: Flow cytometer gating strategy for satellite cell sorting after digestion with 600 µL of

Liberase TL. (**A**) Selection of the population of interest based on FSC-A and SSC-A parameters. (**B**) Single cell identification based on FSC-A and FSC-H. (C) Identification of living cells with FVS 780. (**D**) Negative cell selection based on CD11b, CD31, CD45, and TER119 antigens. (**E-F**) Positive cell selection based on CD34 and ITGA7 (**E**) as well as CXCR4 (**F**) antigens. Gates are represented as black boxes. Please click here to download this File.

Supplementary Figure 4: Characterization of H3K4me2, H3K27ac, and AR genomic locations. (**A**) Pie charts depicting the peak distribution of H3K4me2, H3K27ac, and AR according to genome features in satellite cells. (**B**) Pie charts depicting the peak distribution of H3K4me2, H3K27ac, and AR according to their distance to the nearest TSS in satellite cells. (**C**) Heatmap showing the Pearson correlation between H3K4me2, H3K27ac, and IgG control. Please click here to download this File.

Supplementary Figure 5: Genomic profiles of satellite cell chromatin at stress-response induced genes. Localization of H3K4me2 and H3K27ac at indicated genes on the chromatin of satellite cells. Immunoprecipitation with IgG was used as a negative control. Please click here to download this File.

Supplementary Figure 6: Genomic profiles of satellite cell chromatin at known AR target genes. Localization of H3K4me2, H3K27ac, and AR at indicated genes on the chromatin of satellite cells determined by CUT&RUN. AR peaks are boxed in blue, and corresponding AR-responsive elements are presented below. CUT&RUN performed with IgG was used as a negative control. Please click here to download this File.

Supplementary Figure 7: Genomic profiles of satellite cell chromatin at their selectively expressed genes. Localization of H3K4me2, H3K27ac, and AR at indicated genes on the chromatin of satellite cells determined by CUT&RUN. AR peaks are boxed in blue, and corresponding AR-responsive elements are presented below. CUT&RUN performed with IgG was used as a negative control. Please click here to download this File.

Discussion

The present study reports a standardized, reliable, and easy-to-perform method for the isolation and culture of mouse satellite cells, as well as the assessment of transcriptional regulation by the CUT&RUN method.

This protocol involves several critical steps. The first is muscle disruption and fiber digestion to ensure a high number of collected cells. Despite the increased enzyme concentration, more living cells were obtained than using Protocol 1. Satellite cells express a specific pattern of various membrane proteins. To increase the stringency of our sorting, we used a combination of previously described negative (CD31, TER119, CD45, and CD11b) and positive (CD34, ITGA7, and CXCR4) satellite cell markers[30,31]. Using this strategy, an average of 1% of living putative satellite cells was obtained. This outcome is in the range of what was expected, since satellite cells represent 2%-7% of muscle cell population at adulthood in mice[32]. As a control for the satellite cell selection markers, CD34+/ITGA7-/CXCR4- cells were isolated. Immunofluorescent staining demonstrated that, whereas CD34+/ITGA7-/CXCR4- cells did not express PAX7, 70% of CD34+/ITGA7+/CXCR4+ sorted cells were positive for this satellite cell-specific marker, thereby demonstrating that the FACS isolated population corresponds to satellite cells. In addition, 70% of satellite

cells grown in myogenic medium for 7 days were PAX7-/DMD +, as shown by immunostaining, and formed an elongated multinucleated myofiber, demonstrating that isolated satellite cells conserved their stemness potential.

The major limitation in sample preparation might be the use of a high concentration of enzymes, which results in a large amount of dissociated biological material, but may contribute to increased cell death. To resolve this issue, an assay requiring lower enzyme quantity was tested. In this context, Liberase TL, a purified form of the traditional collagenase[33], was tested. Although digestion was apparently more efficient with this enzyme, the amount of cell debris remained elevated, and the cell viability was slightly lowered. These observations are in agreement with previous reports that compared Liberase-mediated tissue digestion to this with recombinant collagenase or custom collagenase[24,25]. In addition, even though the proportion of endothelial and immune cells was similar between collagenase and Liberase digestion, the percentage of satellite cells was lower in the Liberase-processed sample, overall showing that Liberase is not recommended for satellite cell isolation. The use of this enzyme is suitable for the phenotypic and quantitative analysis of immune cells and could eventually be recommended in the context of muscle and/or other tissues. This is in concordance with what has been reported on Liberase TL as the most suited to effectively isolate viable immune cells[34,35,36].

Another potential issue is the stress caused by both dissociating and sorting satellite cells. However, the absence of H3K27ac and the low H3K4me2 levels at the promoter region of stress response genes identified by single-cell RNA sequencing in mouse satellite cells[26] show that the procedure is mild enough not to induce the stress response transcriptional repertoire. Other limitations to be noted are the selected antigens that remain empiric. However, studies show a high overlap between unique surface marker combinations that are enriched for skeletal muscle satellite cells[30,31].

An additional critical step is the purification of nuclei from sorted cells. For this, the sorting speed is maintained low in order not to damage the cells, but fast enough that they are not stored for too long in FACS buffer. Indeed, CUT&RUN nuclei are not fixed, and a longer incubation time might influence the read obtained from the protocol. A typical preparation from the two hind limbs of one mouse allows CUT&RUN with one antibody and one IgG control, with an amount of 2.5 ng of chromatin for each.

CUT&RUN experiments, designed to assess transcription factor binding and epigenetic modifications, provided strong and robust read signals for H3K4me2 and H3K27ac. The high read levels of H3K4me2 and H3K27ac on genes that are known to be expressed in satellite cells, compared to genes expressed in immune or endothelial cells as well as in myofibers, showed that the signal was amplified predominantly from the satellite cells nuclei. In addition, this protocol made the identification of the cistrome of the AR in muscle stem cells possible, which to date remains a technical issue inherent to the poor quality of mouse AR antibodies and the low AR expression levels in cells that are not highly androgen-sensitive, such as epithelial prostate cells. The data presented here unveiled AR-bound regions with high confidence peak scores. As only one replicate was originally assessed per antibody, the robustness of our datasets will be improved by adding at least two additional biological replicates per condition. However, AR known target genes and respective histone marks, originally described as highly

expressed and/or easily detectable in other tissue contexts such as the prostate, present lower expression levels and are very challenging to detect in satellite cells.

One limitation of the CUT&RUN approach is that it is performed in unfixed cells. Thus, we might have missed some AR targets because of the labile nature of the interactions between transcription factors and their binding site. Similarly, some post-translational modifications, such as acetylation, can also be rather labile. Therefore, including a light fixation step with formaldehyde or paraformaldehyde, after FACS sorting, and before isolating the nuclei, could be considered to stabilize the protein/DNA interactions and histone modifications.

Although this paper shows that CUT&RUN assays can be conducted on FACS-isolated satellite cells, other analyses that use non-fixed chromatin such as ATAC-seq might also be performed. In addition, even though here muscles were harvested in basal physiological conditions, this protocol may be applied to pathological contexts such as injury or aging. All these protocol uses will allow a detailed understanding of gene regulatory mechanisms in satellite cells, and may help in understanding how these mechanisms might be altered by pathophysiological conditions.

In summary, this low-cost and time-efficient protocol provides an effective experimental setting to study transcription factor recruitment and chromatin landscape in skeletal muscle precursor cells. Chromatin prepared by this protocol has provided the first genome-wide analysis of AR cistrome in satellite cells and will facilitate future studies on gene regulation.

Disclosures

The authors declare that they have no competing financial interests.

Acknowledgments

We thank Anastasia Bannwarth for providing excellent technical assistance. We thank the IGBMC animal house facility, the cell culture, the Mouse Clinical Institute (ICS, Illkirch, France), the imaging, the electron microscopy, the flow cytometry, and the GenomEast platform, a member of the 'France Génomique' consortium (ANR-10-INBS-0009).

This work of the Interdisciplinary Thematic Institute IMCBio, as part of the ITI 2021-2028 program of the University of Strasbourg, CNRS and Inserm, was supported by IdEx Unistra (ANR-10-IDEX-0002) and by SFRI-STRAT'US project (ANR 20-SFRI-0012) and EUR IMCBio (ANR-17-EURE-0023) under the framework of the French Investments for the Future Program. Additional funding was delivered by INSERM, CNRS, Unistra, IGBMC, Agence Nationale de la Recherche (ANR-16-CE11-0009, AR2GR), AFM-Téléthon strategic program 24376 (to D.D.), INSERM young researcher grant (to D.D.), ANR-10-LABX-0030-INRT, and a French State fund managed by the ANR under the frame program Investissements d'Avenir (ANR-10-IDEX-0002-02). J.R. was supported by the Programme CDFA-07-22 from the Université franco-allemande and Ministère de l'Enseignement Supérieur de la Recherche et de l'Innovation, and K.G. by the Association pour la Recherche à l'IGBMC (ARI).

References

1. Frontera, W. R., Ochala, J. Skeletal muscle: a brief review of structure and function. *Calcified Tissue International.* **96** (3), 183-195 (2015).

2. Tedesco, F. S., Dellavalle, A., Diaz-Manera, J., Messina, G., Cossu, G. Repairing skeletal muscle: regenerative potential of skeletal muscle stem cells. *The Journal of Clinical Investigation.* **120** (1), 11-19 (2010).
3. Mauro, A. Satellite cell of skeletal muscle fibers. *The Journal of Biophysical and Biochemical Cytology.* **9** (2), 493-495 (1961).
4. Buckingham, M. Skeletal muscle progenitor cells and the role of Pax genes. *Comptes Rendus Biologies.* **330** (6-7), 530-533 (2007).
5. Tosic, M. et al. Lsd1 regulates skeletal muscle regeneration and directs the fate of satellite cells. *Nature Communications.* **9** (1), 366 (2018).
6. Kuang, S., Gillespie, M. A., Rudnicki, M. A. Niche regulation of muscle satellite cell self-renewal and differentiation. *Cell Stem Cell.* **2** (1), 22-31 (2008).
7. Collins, C. A. et al. Stem cell function, self-renewal, and behavioral heterogeneity of cells from the adult muscle satellite cell niche. *Cell.* **122** (2), 289-301 (2005).
8. Robinson, D. C. L. et al. Negative elongation factor regulates muscle progenitor expansion for efficient myofiber repair and stem cell pool repopulation. *Developmental Cell.* **56** (7), 1014-1029, (2021).
9. Machado, L. et al. In situ fixation redefines quiescence and early activation of skeletal muscle stem cells. *Cell Reports.* **21** (7), 1982-1993 (2017).
10. Hainer, S. J., Fazzio, T. G. High-resolution chromatin profiling using CUT&RUN. *Current Protocols in Molecular Biology.* **126** (1), e85 (2019).
11. Meers, M. P., Bryson, T. D., Henikoff, J. G., Henikoff, S. Improved CUT&RUN chromatin profiling tools. *eLife.* **8**, (2019).
12. Gunther, S. et al. Myf5-positive satellite cells contribute to Pax7-dependent long-term maintenance of adult muscle stem cells. *Cell Stem Cell.* **13** (5), 590-601 (2013).
13. Donlin, L. T. et al. Methods for high-dimensional analysis of cells dissociated from cryopreserved synovial tissue. *Arthritis Research & Therapy.* **20** (1), 139 (2018).
14. Rico, L. G. et al. Accurate identification of cell doublet profiles: Comparison of light scattering with fluorescence measurement techniques. *Cytometry. Part A.* **103** (3), 447-454 (2022).
15. Schreiber, V. et al. Extensive NEUROG3 occupancy in the human pancreatic endocrine gene regulatory network. *Molecular Metabolism.* **53**, 101313 (2021).
16. Rovito, D. et al. Myod1 and GR coordinate myofiber-specific transcriptional enhancers. *Nucleic Acids Research.* **49** (8), 4472-4492 (2021).
17. Langmead, B., Salzberg, S. L. Fast gapped-read alignment with Bowtie 2. *Nature Methods.* **9** (4), 357-359 (2012).
18. Meers, M. P., Tenenbaum, D., Henikoff, S. Peak calling by Sparse Enrichment Analysis for CUT&RUN chromatin profiling. *Epigenetics Chromatin.* **12** (1), 42 (2019).
19. Ramirez, F. et al. deepTools2: a next generation web server for deep-sequencing data analysis. *Nucleic Acids Research.* **44** (W1), W160-W165 (2016).
20. Thorvaldsdottir, H., Robinson, J. T., Mesirov, J. P. Integrative Genomics Viewer (IGV): high-performance genomics data visualization and exploration. *Briefings in Bioinformatics.* **14** (2), 178-192 (2013).
21. Heinz, S. et al. Simple combinations of lineage-determining transcription factors prime cis-regulatory

elements required for macrophage and B cell identities. *Molecular Cell.* **38** (4), 576-589 (2010).

22. Zou, Z., Ohta, T., Miura, F., Oki, S. ChIP-Atlas 2021 update: a data-mining suite for exploring epigenomic landscapes by fully integrating ChIP-seq, ATAC-seq and Bisulfite-seq data. *Nucleic Acids Research.* **50** (W1), W175-W182 (2022).
23. Liu, L., Cheung, T. H., Charville, G. W., Rando, T. A. Isolation of skeletal muscle stem cells by fluorescence-activated cell sorting. *Nature Protocols.* **10** (10), 1612-1624 (2015).
24. Brandhorst, H. et al. Successful human islet isolation utilizing recombinant collagenase. *Diabetes.* **52** (5), 1143-1146 (2003).
25. Nikolic, D. M. et al. Comparative analysis of collagenase XI and liberase H1 for the isolation of human pancreatic islets. *Hepatogastroenterology.* **57** (104), 1573-1578 (2010).
26. Machado, L. et al. Tissue damage induces a conserved stress response that initiates quiescent muscle stem cell activation. *Cell Stem Cell.* **28** (6), 1125-1135, (2021).
27. Diel, P., Baadners, D., Schlupmann, K., Velders, M., Schwarz, J. P. C2C12 myoblastoma cell differentiation and proliferation is stimulated by androgens and associated with a modulation of myostatin and Pax7 expression. *Journal of Molecular Endocrinology.* **40** (5), 231-241 (2008).
28. Gronemeyer, H., Gustafsson, J. A., Laudet, V. Principles for modulation of the nuclear receptor superfamily. *Nature Reviews Drug Discovery.* **3** (11), 950-964 (2004).
29. Billas, I., Moras, D. Allosteric controls of nuclear receptor function in the regulation of transcription. *Journal of Molecular Biology.* **425** (13), 2317-2329 (2013).
30. Garcia-Prat, L. et al. FoxO maintains a genuine muscle stem-cell quiescent state until geriatric age. *Nature Cell Biology.* **22** (11), 1307-1318 (2020).
31. Maesner, C. C., Almada, A. E., Wagers, A. J. Established cell surface markers efficiently isolate highly overlapping populations of skeletal muscle satellite cells by fluorescence-activated cell sorting. *Skeletal Muscle.* **6**, 35 (2016).
32. Schultz, E. A quantitative study of the satellite cell population in postnatal mouse lumbrical muscle. *The Anatomical Record.* **180** (4), 589-595 (1974).
33. Hyder, A. Effect of the pancreatic digestion with liberase versus collagenase on the yield, function and viability of neonatal rat pancreatic islets. *Cell Biology International.* **29** (9), 831-834 (2005).
34. Liang, F. et al. Dissociation of skeletal muscle for flow cytometric characterization of immune cells in macaques. *Journal of Immunological Methods.* **425**, 69-78 (2015).
35. Park, J. Y., Chung, H., Choi, Y., Park, J. H. Phenotype and tissue residency of lymphocytes in the murine oral mucosa. *Frontiers in Immunology.* **8**, 250 (2017).
36. Skulska, K., Wegrzyn, A. S., Chelmonska-Soyta, A., Chodaczek, G. Impact of tissue enzymatic digestion on analysis of immune cells in mouse reproductive mucosa with a focus on gammadelta T cells. *Journal of Immunological Methods.* **474**, 112665 (2019).